Molecular Crystals and Liquid Crystals

Publication details, including instructions for authors and subscription information:
http://www.tandfonline.com/loi/gmcl20

NMR Study of Slow Motions of HDA Hydrocarbons Chains Inside Lamellar Structures

J. Schneider [a] , L. V. S. Lopes [a] , C. E. Tambelli [a] , J. P. Donoso [a] , H. Lozano [b] & G. González [b]

[a] IFSC, Universidade de São Paulo, São Carlos, SP, Brasil

[b] Depto. de Química, Facultad de Ciencias, Universidad de Chile, Santiago, Chile

Version of record first published: 16 Jun 2008

To cite this article: J. Schneider, L. V. S. Lopes, C. E. Tambelli, J. P. Donoso, H. Lozano & G. González (2008): NMR Study of Slow Motions of HDA Hydrocarbons Chains Inside Lamellar Structures, Molecular Crystals and Liquid Crystals, 483:1, 130-140

To link to this article: http://dx.doi.org/10.1080/15421400801904336

Mol. Cryst. Liq. Cryst., Vol. 483, pp. 130–140, 2008

ISSN: 1542-1406 print/1563-5287 online
DOI: 10.1080/15421400801904336

Taylor & Francis
Taylor & Francis Group

NMR Study of Slow Motions of HDA Hydrocarbons Chains Inside Lamellar Structures

J. Schneider[1], L. V. S. Lopes[1], C. E. Tambelli[1], J. P. Donoso[1], H. Lozano[2], and G. González[2]
[1]IFSC, Universidade de São Paulo, São Carlos, SP, Brasil
[2]Depto. de Química, Facultad de Ciencias, Universidad de Chile, Santiago, Chile

Measurements of ^{1}H and ^{13}C Nuclear Magnetic Resonance (NMR) for the nanocomposite materials formed by the intercalation of hexadecylamine (HDA) in metal oxides (TiO_2, V_2O_5 and MoO_3), are reported. The ^{1}H NMR spin-lattice relaxation in the rotating frame was described by using the spectral density due to Davidson and Cole, which incorporates a distribution of correlation times characterized by a width parameter ε. The fitting of the data was obtained for $\varepsilon = 0.74$, indicating that the correlation times are distributed over a narrow range in this system. High-resolution ^{13}C NMR techniques were used to resolve the NMR lines of middle-chain methylene groups in the spectra and variable contact time cross-polarization $\{^{1}H\text{-}\}^{13}C$ experiments were employed to analyze the reorientation dynamics of the CH_3 and CH_2 groups in the HDA chains.

Keywords: foam; hexadecylamine; intercalation compound; nanostructure; NMR

INTRODUCTION

The hybrid organic–inorganic compounds derived from metal oxides have been drawing attention on account of their ionic and electronic properties leading to potential applications in solid-state lithium batteries, sensors, smart windows, catalysis and electrochromic devices [1–5]. Among these materials, the metal oxide foams described by Chandrappa et al. [6] have been the object of a great deal of research. These authors synthesized macroporous V_2O_5-amine composites in a

Partial support of Capes, CNPq, FAPESP and PRONEX /FAPESP / CNPq (Grant 03/09859-2) and FONDECYT (Grants 105344 and 7070308) are gratefully acknowledged.

Address correspondence to J. P. Donoso, Instituto de Física de São Carlos, Universidade de São Paulo, PO Box 369, 13560-970 São Carlos, SP, Brasil. E-mail: donoso@if.sc.usp.br

single step reaction by intercalation of hexadecylamine (HDA) into layered V_2O_5 in the presence of hydrogen peroxide by using the exothermic reaction between amines and H_2O_2 [5]. The synthesis of TiO_2-foams by the same effervecent reaction of hydrogen peroxide inside a metal oxide containing intercalated alkylamine was reported by Arabatzis and Falaras [7]. Amines are excellent guest molecules which can easily be intercalated into the interlayer spaces of inorganic materials. The intercalation of long chain alkyl amine molcules into metal oxides leads to the formation of lamellar nanostructures.

In a previous paper we reported measurements ^1H and ^{13}C Nuclear Magnetic Resonance (NMR) for the nanocomposite materials formed by the intercalation of HDA into TiO_2 and MoO_3. We proposed a possible attribution of the ^{13}C lines in the high-resolution NMR spectra and we examined the temperature dependence of the proton (^1H) NMR spectra shape. The ^1H NMR relaxation was found to be nonexponential probably resulting from the complexity of the HDA chain segments motions in these systems. [8].

In the present work, we report a proton (^1H) and carbon (^{13}C) nuclear magnetic resonance (NMR) investigation of the conformational and dynamical properties of oxide foams derived from hexadecylamine (HDA) intercalated in metal oxides (TiO_2, V_2O_5 and MoO_3). The lamellar structure of the nanocomposites was evidenced by Scanning electron microscopy and X-ray diffraction (XRD) measurements. Basal distances of 48 Å, 44 Å and 47 Å were obtained from the XRD data for the MoO_3-HDA, TiO_2-HDA, and the V_2O_5-HDA nanocomposites, respectively. High-resolution ^{13}C-NMR spectra were taken in three different conditions: direct ^{13}C polarization, cross polarization $\{^1H\}-^{13}C$ and ^{13}C direct polarization with high power proton decoupling. The proton relaxation in the rotating frame was analyzed by assuming a distribution of correlation times.

EXPERIMENTAL

The synthesis of the nanocomposites were achieved by the direct decomposition of hydrogen peroxide inside a metal oxide/HDA. nanocomposite Further details of the sample preparation procedure are given elsewhere [8]. Proton (^1H) NMR line shape and spin-lattice relaxation experiments were carried out in powder samples from 170 to 370 K using a pulsed NMR spectrometer operating at 36 MHz. The spin-lattice relaxation time in the rotating frame, $T_{1\rho}$, was measured with a rotating field strength of 18 G. The high-resolution ^{13}C NMR measurements were performed at a magnetic field of 9.4 T (100.6 MHz for ^{13}C) on a Varian Unity Inova spectrometer, using a

7 mm Magic Angle Spinning (MAS) probe. Tetramethylsilane (TMS) was used as a reference for ^{13}C chemical shifts. Samples were spun up to 5.5 KHz in silicon nitride rotors. Spectra were measured with a single pulse excitation and also by $\{^1H\}$-^{13}C cross-polarization (CP) technique. The CP experiment was carried out using a $\pi/2$ ^1H pulse of 3.5 μs, contact time of 1ms, recycle delay of 30 s and ^1H spin lock field of 60 KHz. Also, variable contact time CP experiments were carried out up to 50ms of contact time. In ^{13}C-NMR single pulse experiments a $\pi/2$ pulse of 3.5 μs was used with recycle delay of 30 s. In all ^{13}C-NMR experiments ^1H decoupling of 80 KHz was used during acquisition. Also, delayed decoupling of ^1H (DD) was used to suppress non-quaternary carbon signals, with a delay time of 150 μs between the end of the excitation pulse and the beginning of the ^1H decoupling irradiation [7].

RESULTS AND DISCUSSION

^1H NMR Spectroscopy

In a previous paper, the experimental proton (^1H) NMR spectra at low temperature were described by a narrow line flanked by a pair of peaks conforming a Pake doublet. The mobility of the proton averages out the dipolar interactions above 200 K and the ^1H line narrows. The temperature dependence of the ^1H spin-lattice relaxation time in the laboratory frame T_1 of the samples HDA:TiO_2, HDA:MoO_3, HDA:V_2O_3 and HAD:Cr_2O_3 indicate that very few protons have rate motion of the order of the Larmor frquency, ω_o (36 MHz) [8]. Measurements of the relaxation time carried out in the rotating frame ($T_{1\rho}$) imply shifts of the Larmor frequency from the MHz regime to the kHz regime, so a nuclear spin relaxation rate maximum can be detected at lower temperature. The relaxation time $T_{1\rho}$ is the time characterizing the recovery of the longitudinal magnetization equilibrium in the rotating frame, i.e., it is the relaxation time when the magnetization is locked along the RF magnetic field H_1 (tipically 5–20 G). Thus, $T_{1\rho}$ is sensitive to low-frequency motions (10–50 kHz) [9]. Measurements of the proton spin-lattice relaxation in the rotating frame ($T_{1\rho}$) were undertaken in the sample HDA: MoO_3 (Fig. 1).

The classical theory of the temperature dependence of the spin-lattice relaxation time is given by Bloembergen-Purcell-Pound (BPP) and assumes non-correlated isotropic random motions, yielding a pair-pair spin correlation function of exponential form, $G(t) = exp(-t/\tau)$, parameterized by the correlation time τ, which defines the time scale for changes of the local magnetic field experienced by the resonant

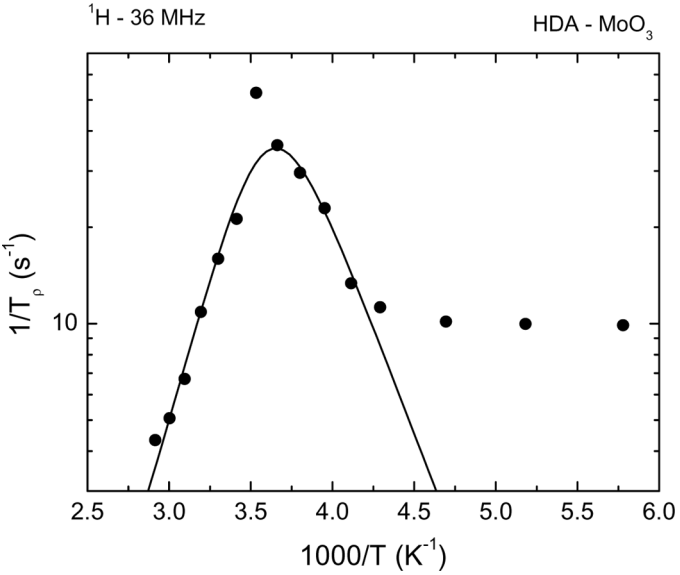

FIGURE 1 Temperature dependence of the ^{1}H spin-lattice relaxation rates in the rotating frame ($T_{1\rho}^{-1}$) in HDA:MoO_3, measured at the frequency $\omega_1 \approx 76$ kHz. Solid lines are the calculated values using the Cole – Davidson spectral density function.

nucleus [9]. In this context, the spectral density function, J(w), given by the Fourier transform of the related correlation function, has a Lorentzian form in the frequency domain

$$J(\omega) = \frac{\tau}{1 + (\omega\tau)^2} \tag{1}$$

The spectral density function is parameterized by the correlation time, τ, of the ionic or molecular motion, modulating the nuclear spin interactions. The spin-lattice relaxation rate in the rotating frame can be expressed in terms of the spectral density function $J(\omega)$ evaluated at the Larmor frequencies in the rotating frame (ω_1) and in the laboratory frame (w_o) of the studied nuclei [10]:

$$\frac{1}{T_{1_\rho}} = C\left[\frac{3}{2}J(2\omega_1) + \frac{5}{2}J(\omega_o) + J(2\omega_o)\right] \tag{2}$$

where the constant C depends on the spin interaction responsible for the relaxation. Equations (1) and (2) can be expressed in a temperature dependent form by assuming a thermally activated process.

An Arrhenius temperature dependence for the correlation time is often assumed, $\tau = \tau_o exp\,(E_A/k_BT)$, were k_B is the Boltzmann constant, E_A, is the activation energy and τ_o is the pre-exponential factor. The activation energy can be calculated from the linear slope of the Arrhenius plot of the $T_{1\rho}^{-1}$ data. The BPP model outlined above predicts a symmetric v-shaped $T_{1\rho}^{-1}$ vs. $1/T$ curve with identical slopes on either the high- or low-temperature side of the $T_{1\rho}^{-1}$ maximum.

Measurements of the proton spin-lattice relaxation in the rotating frame ($T_{1\rho}$) were undertaken between 173 and 350 K using a lock field $H_1 \approx 18$ G in the sample HDA:MoO_3 (Fig. 1). The $T_{1\rho}^{-1}$ displays an asymmetrical maxima, where the activation energy obtained from the high temperature side of the rate maximum is greater than that obtained from the low one.

Deviations from the BPP theory, frequently encountered in nuclear relaxation studies, have been explained in terms of the non-exponentiality of the spin correlation function, which reflects a distribution of motional processes [11]. The ^{1}H NMR relaxation curve in Figure 1 reflects the complexity of the chain segment motions in the nanocomposite and suggests that the correlation function is non exponential because there exists a distribution of correlation times. The restriction imposed by the anchoring of the HDA head group leads to anisotropic chain segments motions [3]. The spectral density due to Davidson and Cole (DC) is one of the most successful spectral densities used to interpret nuclear spin relaxation experiments [12]. It incorporates a distribution of correlation times characterized by a width parameter ε, whith $0 < \varepsilon \leq 1$.

$$J_{DC} = \frac{2}{\omega}\left\{\frac{\sin[\varepsilon \arctan(\omega\tau)]}{(1+\omega^2\tau^2)^{\varepsilon/2}}\right\} \tag{3}$$

The slope on the high-temperature side of the $T_{1\rho}^{-1}$ maximum is E_A and on the low-temperature side is $-\varepsilon E_A$. For $\varepsilon = 1$, the DC distribution function turns into the Poisson distribution specified by one correlation time. As a result, the BPP spectral density and hence a symmetrical curve are obtained. The solid line in Figure 1 shows the fitting of the data by the Davidson and Cole spectral density, Eq. (3), using $E_A = 0.36$ eV, $\tau_o \approx 3 \times 10^{-13}$ s and $\varepsilon = 0.74$. This approach, which leads to a useful parametrization of the ^{1}H NMR data is consistent with the picture that the relative motional correlation times of the hydrogen atoms along the intercalated amine chains is well described by a distribution of correlation times. The parameter ε characterizing the distribution of correlation times is relatively large

($\varepsilon = 0.74$) indicating that the correlation times are distributed over a narrow range in this system. Equations (2) and (3) predict a maximum in $T_{1\rho}^{-1}$ when 2 $\omega_1\tau \approx 1$. Therefore, the position of the relaxation rate maximum $(T_{1\rho}^{-1})_{max}$indicates the temperature T_{max} at which the motional correlation time is comparable to the reciprocal of the ^{1}H Larmor frequency in the lock field H_1, e.i. $\tau = (2\omega_1)^{-1} = (2\gamma H_1)^{-1} \approx 10^{-6}$ s, where γ is the proton gyromagnetic ratio. This result indicates that most of the protons of the HDA chain in the HDA: MoO_3 nanocomposite have a relatively low mobility.

^{13}C High-Resolution NMR Spectroscopy

Figures 2, 3 and 4 shows the high-resolution ^{13}C-NMR spectra for the composites with Mo, V and Ti, respectively. Three kinds of ^{13}C-NMR experiments are shown. The upper trace in each figure corresponds to single pulse experiments, the middle trace to CP $\{^1H\}-^{13}C$ experiments with 1ms of contact time and the lower trace to single pulse DD experiments with 150 μs delay. Combining the complementary CP and DD spectra, where signals are respectively enhanced and attenuated according to the strength of the dipolar coupling, it is possible to resolve more NMR lines of middle-chain methylene groups than in any single spectrum. Table 1 shows the chemical shift from the resolved lines in each compound and their corresponding attributes. The methlyene C with the lowest chemical shift, 23.4 ppm, corresponds to the carbon bonded to CH_3. The Mo compound shows the most resolved NMR spectra of the series, indicating well defined structural environments for the HDA molecules. Conversely, the V compound shows the broadest NMR lines of the series, indicating loosely defined structural environments. On the other hand, there are differences in the reorientation dynamics of the CH_3 groups. The significant intensity of the CH_3 line in the DD spectrum of the Mo compound indicates a rapid reorientation, reducing the effective $^1H-^{13}C$ dipolar coupling. In the Ti compound the reorientation may be less rapid, due to the relative increase in CP signal. In the V compound, the reorientation of the CH_3 is the most hindered of the set of samples, as can be inferred from the weakest intensity for this signal measured in the DD spectra.

Figure 5 shows the results from variable contact time cross-polarization $\{^1H-\}^{13}C$ experiments. Only the intensities of the three strongest and best resolved signals in the CP spectra were plotted: the CH_3, and two of the CH_2 lines, centered at approximately 24 ppm and 33 ppm. There is a significant difference among these curves. The

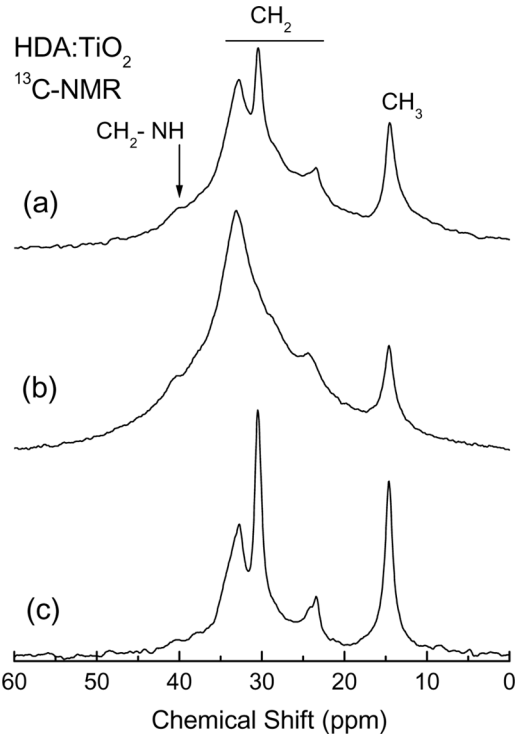

FIGURE 2 ^{13}C-NMR spectra for the HDA:TiO_2 complex. (a) Single pulse experiment with ^{1}H decoupling. (b) $\{^{1}H\}-^{13}C$ cross-polarization experiment. (c) Single pulse with delayed ^{1}H decoupling.

Mo compound shows the slowest increase in ^{13}C polarization (Fig. 5(c)), indicating the weakest $^{1}H-^{13}C$ dipolar coupling in the set of compounds. The evolution of the ^{13}C magnetization as a function of the contact time was analyzed according to the expression for CP from an abundant spin reservoir (^{1}H) and radio frequency fields close to the Hartmann-Hahn match condition [13]:

$$M(t) = \frac{M_O}{1 - T_{HC}/T_{1\rho}^{H}} \left(1 - \exp\left(- \frac{t}{T_{HC}\left(1 - T_{HC}/T_{1_\rho}^{H}\right)} \right) \right) \exp\left(- \frac{t}{T_{1_\rho}^{H}} \right) \tag{4}$$

where M_o is an amplitude factor, T_{H-C} is the characteristic contact time of magnetization transfer from ^{1}H to ^{13}C and $T_{1\rho}^{H}$ is the spin-lattice relaxation time for ^{1}H in the rotating frame. Least-square fittings of

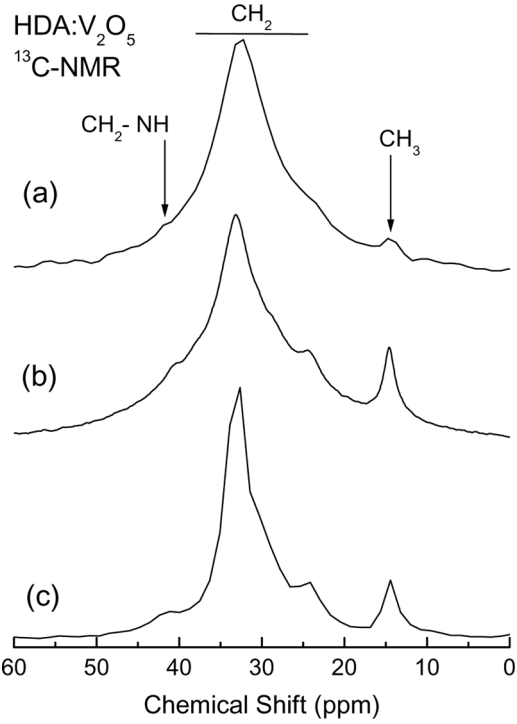

FIGURE 3 ^{13}C-NMR spectra for the HDA:V_2O_5 complex. (a) Single pulse experiment with ^{1}H decoupling. (b) $\{^1H\}-^{13}C$ cross-polarization experiment. (c) Single pulse with delayed ^{1}H decoupling.

this expression were carried out in order to quantify the characteristic times for the CP transfer in each compound. Table 2 shows the obtained parameters. In the case of the Mo-complex, the $T_{1\rho}^H$ could not be calculated because it is longer than the maximum possible contact time allowable in the NMR probe (50 ms). As can be seen, the T_{H-C} values are two orders of magnitude longer in the Mo-complex than in the other two compounds. This is a direct evidence of the weak ^{1}H-^{13}C dipolar interactions in this complex, related to a rapid fluctuation in the direction of the $^1H-^{13}C$ internuclear vectors. The very short T_{H-C} values measured for the V and Ti complexes point to strong intra and intermolecular $^1H-^{13}C$ couplings and, therefore, dynamically restricted methylene chains. Also, the $T_{1\rho}^H$ values in these two compounds are substantially shorter than in the Mo-complex for the same H_1 lock field

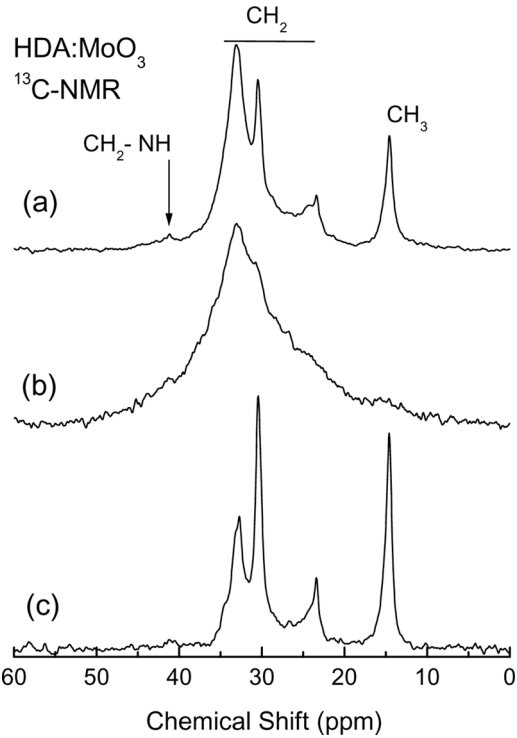

FIGURE 4 ^{13}C-NMR spectra for the HDA:MoO_3 complex. (a) Single pulse experiment with ^{1}H decoupling. (b) $\{^1H\}-^{13}C$ cross-polarization experiment. (c) Single pulse with delayed ^{1}H decoupling.

TABLE 1 Identification of ^{13}C-NMR Lines in the Complexes

Line identification	MO_3-HDA δ (ppm)	V_2O_5-HDA δ(ppm)	TiO_2-HDA δ (ppm)
CH_3	14.6	14.4	14.5
CH_2	23.4		23.4
CH_2	24.2	24.4	24.2
CH_2	26.7		
CH_2	28.7	28.9	
CH_2	30.5		30.0
CH_2	32.7		32.8
CH_2	33.1	33.2	
CH_2	34.4		
CH_2-NH_2	41.2	40.3	40.0

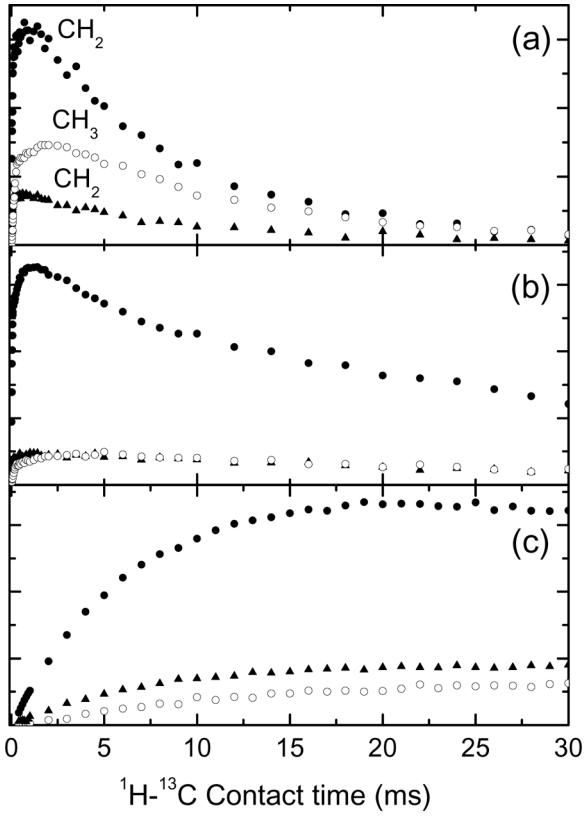

FIGURE 5 ^{13}C Magnetization in variable contact time cross-polarization $\{^1H-\}^{13}C$ experiments for CH_3 (hollow circles), and two of the resolved CH_2 lines, centered at 24 ppm (black triangles) and 33 ppm (black circles). (a) HDA:TiO_2, (b) HDA:V_2O_5, (c) HDA:MoO_3. Data were acquired up to contact times of 50 ms in all experiments.

TABLE 2 Characteristic Times for $\{^1H\}-^{13}C$ Cross-Polarization NMR of the Main Resonance Lines, Extracted from the Variable Contact Time Experiments

Line	Times	MO_3-HDA	V_2O_5-HDA	TiO_2-HDA
CH_3	T_{HC} (ms)	14 ± 2	0.36 ± 0.04	0.25 ± 0.02
	$T^H_{1\rho}$ (ms)	—	47 ± 4	14 ± 1
CH_2	T_{HC} (ms)	8.8 ± 0.3	0.056 ± 0.007	0.052 ± 0.003
(24 ppm)	$T^H_{1\rho}$ (ms)	190 ± 20	45 ± 3	11 ± 1
CH_2	T_{HC} (ms)	7.3 ± 0.1	0.053 ± 0.004	0.067 ± 0.004
(33 ppm)	$T^H_{1\rho}$ (ms)	113 ± 3	33 ± 1	11 ± 1

for ^{1}H of 60 kHz, indicating a strong coupling of the ^{1}H reservoir with the lattice.

CONCLUSIONS

The temperature dependence of the ^{1}H NMR spin-lattice relaxation in the rotating frame was measured for the nanocomposite formed by the intercalation of hexadecylamine in MoO_3. A Davidson – Cole distribution of correlation times was used to analyse the ^{1}H relaxation data. In these nanocomposites, the proton (and the carbon) mobility depends on the position in the HDA hydrocarbon chain due to the restriction imposed by the anchoring of the head group. From the high-resolution ^{13}C-NMR experiments, it was concluded that the mobility of the HDA molecular fragments in the Mo complex is the highest of the set, for both CH_2 and CH_3 groups. In V and Ti complexes, the molecular mobility is severely restricted. Such a behavior may be understand by considering that of these three oxides only the MoO_3 has an intrinsic laminar structure.

REFERENCES

[1] Carn, F., Steunou, N., Livage, J., Colin, A., & Backov, R. (2005). *Chem. Mater.*, *17*, 644.
[2] Surnev, S., Ramsey, M. G., & Netzer, F. P. (2003). *Progr. Surface Science*, *73*, 117.
[3] Durupthy, O., Jaber, M., Steunou, N., Maquet, J., Chandrappa, G. T., & Livage, J. (2005). *Chem. Mater.*, *17*, 6395.
[4] Krawiec, P., De Cola, P. L., Gläser, R., Weitkamp, J., Weidenthaler, C., & Kaskel, S. (2006). *Advanced Materials*, *18*, 505.
[5] Shukoor, M. I., Therese, H. A., Gorgishvili, L., Glasser, G., Kolb, U., & Tremel, W. (2006). *Chem Mater.*, *18*, 2144.
[6] Chandrappa, G. T., Steunou, N., & Livage, J. (2002). *Nature*, *416*, 702.
[7] Arabatzis, I. M. & Falaras, P. (2003). *Nano Letters*, *3*, 249.
[8] Lopes, L. V. S., Schneider, J., Magon, C. J., Donoso, J. P., Lozano, H., & Gonzalez, G. (2006). *Molecular Crystals & Liquid Crystals*, *448*, 187–195.
[9] Abragam, A. (1961). *Principles of Nuclear Magnetism*, Oxford University: London.
[10] Boyce, J. B. & Huberman, B. A. (1979). *Physics Reports*, *51*, 189.
[11] Donoso, J. P., Bonagamba, T. J., Panepucci, H. C., Oliveira, L. N., Gorecki, W., Berthier, C., & Armand, M. (1993). *J. Chemical Physics*, *98*, 10026.
[12] Beckmann, P. A. (1988). *Physics Report*, *171*, 85.
[13] Mehring, M. (1983). *Principles of High Resolution NMR in Solids*, Springer-Verlag: Berlin, Second Edition.